Propagation Losses of UWB Antenna for On-Body to In-Body Signal Propagation

A. Priya[1], S. Kaja Mohideen[1], and P. Thirumaraiselvan[2, *]

Abstract—To provide better care to the people, who are living in rural areas and whoever in need of emergency medical care, it becomes essential to develop remote monitoring health care applications. Body Area Networks (BAN) that are formed with wearable or implanted wireless sensor devices will play an important role to achieve the above task. Since the communication in BAN is of short communication distance and higher data rate, the Ultra-Wideband (UWB) radio signals make themselves as the right candidates due to their inherent characteristics. This requires more research in design and development of UWB transceivers, especially for implantable biomedical devices. This paper proposes a UWB antenna design and a numerical channel model to predetermine the path loss characteristics of an on-body to in-body channel in UWB. The proposed model has been developed using ray tracing procedures and includes the antenna polarization and radiation pattern. In addition, the predicted results have been validated by measurements conducted with honey based liquid phantoms.

1. INTRODUCTION

Remote monitoring of patient status with Body Area Networks (BAN) enables monitoring the patients wirelessly even in intensive care units or operation theatre and make the life easier for patients and doctors. Hence, monitoring bio-potential signals in real time is getting a lot of attention nowadays. Generally, BAN is formed with wearable or implanted wireless sensor devices. In a BAN, the communication is in short range and with high data rate. Since the Ultra-Wideband (UWB) exhibits noise like behaviour, it is found much suitable for this application. Detecting UWB signals is difficult. They are robust to jamming, and hence, implementation of complex data encryption process in transceivers is not necessary [1]. In addition, interference due to radio signals from UWB transmitters to other radio devices is not very significant. Since the power level of UWB signals is less than the noise floor, it will not be a threat to human [2].

However, the UWB is not standardized in the frequency allocation for medical applications, especially for implantable biomedical devices. With the development of miniaturized, low power, UWB transceiver is practically feasible, and high data rate applications such as Capsule Endoscopy, targeted drug delivery systems, biopsy and therapeutic diagnosis using micro robots are going to play a vital role in the future e-health systems [3]. This requires more attention in the design and development of implantable sensors with wireless transceivers and better understanding of radio signal propagation through human tissues in UWB. Designing an antenna with stable and omnidirectional radiation properties in the entire UWB band is of vital importance, and achieving all these with fine tuning of the feed is reported in [4]. Printed slot antennas of elliptical and circular slot antennas with feeds on the same side and different sides are presented for UWB applications in [5]. Enhancing the bandwidth is a major factor in an antenna design. A fractal implementation of an antenna will report at least

twice an impedance bandwidth improvement compared to conventional printed slot antennas [6]. Since measurement of radio signals inside living human bodies is not practically feasible, development of channel models to predict the signal propagation inside the human body is becoming essential nowadays. Many BAN channel measurements and models have been published in the past, and most of them have characterized ISM and other narrow band channels. Though significant efforts have been found in the UWB channel characterization, to the best of the knowledge of the authors, very few models have been proposed to characterize the UWB propagation with implantable sensors. The very first UWB channel model, which investigated the feasibility of using 3.4–4.8 GHz lower UWB as a wireless link between in-body and on-body transceivers is [7]. To derive this model, numerical simulations were conducted with a frequency dependent finite difference time domain (FDTD) method in combination with a voxel model [8] of an adult male. This voxel model is available at the National Institute of Information and Communications Technology in Japan. It was developed based on magnetic resonance imaging (MRI) data and included almost 50 types of tissues. Implanted sensing devices were assumed at 20 arbitrary locations within the chest to a depth between 6 mm and 18 mm during the numerical simulations.

Since numerical simulations consume more time and require composite human models, a statistical channel model has been proposed in [9] and [10] for 1–6 GHz at a depth between 5 and 120 mm in the chest. However, initially simulations were performed using time-domain finite integration techniques (FIT) with a voxel model of the human body, which was described by the frequency dependent dielectric properties as given in the Gabriel database [11]. Then by analyzing the simulation results the above statistical model was proposed. It was further improved by incorporating frequency dependent attenuation in [12]. Another statistical channel model has also been proposed for in-body to on-body propagation in the abdomen region in between 1–6 GHz [13]. The locations of the implanted devices have been fixed in the abdomen of the anatomical model that was used for numerical simulations. The channel path losses of in-body probes were computed at 10–150 mm inside the human abdomen and analyzed in order to derive this particular model. The above model was also improved by the same authors by including the computational analysis and path loss in the digestive tract in between 3.4–4.8 GHz so that it could be applied to capsule endoscopy [14]. The first UWB path loss model for in-body to on-body was developed from in-vivo measurements taken in anesthetized porcine subject and is found in the literature [15]. This proposed path loss model works well for implantation depths of 5–16 cm and within 1–6 GHz.

At the in body communication environment of a body area network with implanted sensors, the transmitted signal undergoes significant signal loss due to multipath propagation through tissue layers and bones. In addition, concrete floors and metal frames that support drop ceilings, which are constructed with acoustical materials, exist in modern hospital buildings. The space inside the rooms may contain beds, metallic tables, trolleys and medical equipment to monitor the status of the patients. All of them introduce attenuation to the radio waves.

This requires the use of numerical simulations which evaluate the path loss for a given set of transmitter and receiver locations according to the dielectric and physical properties of off-body structures and of the surrounding tissues, where the transceivers are located. Since site specific information could not be ignored in the prediction of signal attenuation in the above case, the authors propose ray tracing method as the best option for numerical simulation.

This paper proposes a novel design of a UWB antenna and studies the path loss characteristics of an on-body to in-body channel using the proposed antenna in honey based liquid phantom. In addition, simulations are performed using BAN sim [19], to predict the path loss in the above scenario for comparison.

2. ANTENNA DESIGN

2.1. Proposed Structure

The front view of the proposed staircase truncated elliptical slot oval patch with an embedded circular slot antenna and back view with a U-shaped feed is shown in Fig. 1. This antenna is designed using FR4 dielectric material of 1.6 mm thickness, $\varepsilon_r = 4.4$ and loss tangent = 0.02. The dimensions of the proposed antenna are tabulated in Table 1. The antenna geometry from [4] is chosen as the reference, and truncation like staircase based on Koch fractal algorithm is done at the bottom corners of the patch
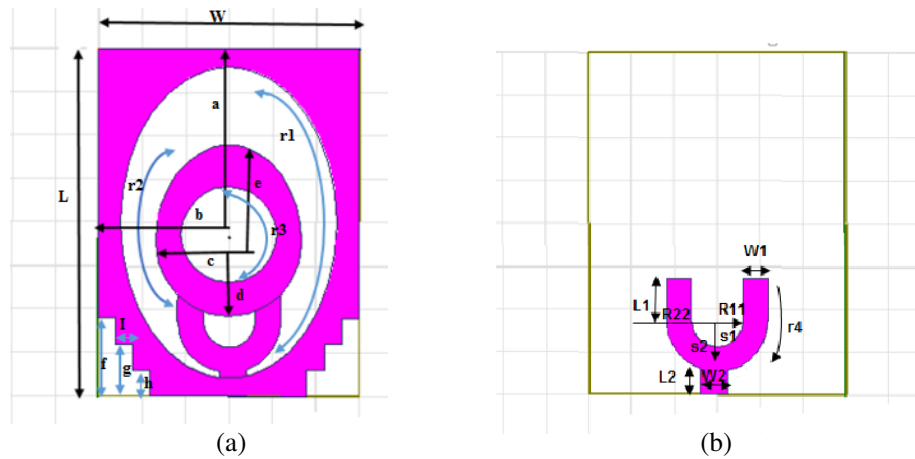
Figure 1. Simulated structure of the proposed staircase truncated UWB antenna. (a) Front side. (b) Back side.

Table 1. Optimized dimensions of the proposed staircase truncated ultra wide band antenna.

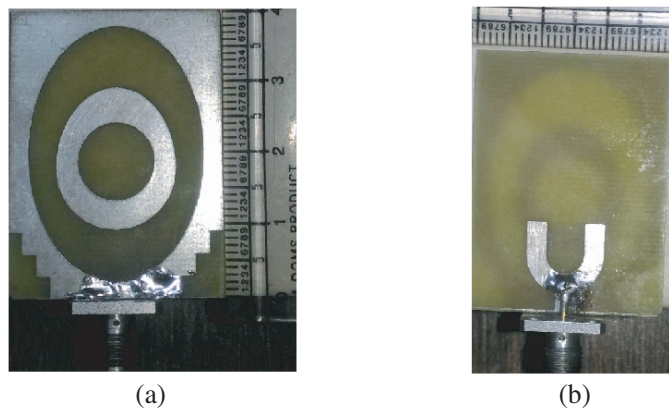| Variables	mm	Variables	mm	Variables	mm	Variables	mm
L	40	e	11.34	h	3	$r4$	12.8
W	30	$r1$	3.14	I	3	$W1$	3
a	17.9	$r2$	6.25	$L1$	5	$W2$	3.2
b	12.45	$r3$	5.5	$L2$	3.35	$S1$	3.14
c	13.5	f	9	$R11$	2.9	$S2$	6.25
d	18.2	g	6	$R22$	5.9		

Figure 2. Prototype of the proposed staircase truncated Ultra Wide band antenna. (a) Front side. (b) Back side.

for the impedance matching and gain enhancement. The dimensions of the oval patch, U-shaped fork, circular slot are optimized iteratively according to the required frequency of operation. The proposed antenna is simulated using a 3D Electromagnetic simulation software HFSS version 13.0, and it is suitable for WLAN and satellite applications. Fig. 2 shows photographs of the fabricated antenna. The U- or fork-shaped feed [4] which is coupled electromagnetically to the front portion excites the patch parasitically. The antenna resonates very well in the UWB from 2 GHz to 10.6 GHz. In the fabricate

prototype a 50 ohm SMA connector is attached to the feed from the back side. There are totally 3 resonant bands within 3.1 GHz to 11 GHz in simulation. The proposed antenna is simulated using HFSS version 13 which is based on FEM analysis method.

2.2. Parametric Analysis

Parametric analysis of the dimensions was done to understand the effect of the staircase truncation and circular slot. When there is no truncation at the bottom corners, the antenna achieves UWB and resonates at three frequencies, but there is a negative gain in the lower resonant band. Following Koch fractal algorithm the first truncation is introduced half way between the middle and the lowermost bottom corner of the patch thus enabling the antenna to resonate at the same operating bands. The second truncation is continued halfway between the first truncation and the bottom corner of the patch and similarly for the third truncation. The number of truncations and the size of the truncation is optimized finally to resonate the antenna for almost the same band of frequencies. The optimized dimensions and the positions of the staircase improve the gain and impedance bandwidth.

2.3. Results and Discussion

The prototype antenna is fabricated on an FR4 substrate having a thickness of 1.6 mm and is tested using Agilent N9925A Vector Network Analyzer (VNA max up to 9 GHz) and calibrated using Agilent 85514A male calibration module. A 3.5 mm diameter SMA type connector is connected to the antenna. The return loss and VSWR of the proposed antenna are measured using VNA in free space condition and in honey phantom, and the measured results are compared with simulated ones as shown in Fig. 3. From Fig. 3, it is observed that the antenna gives a -10 dB return loss from 2 GHz to 11 GHz band. The return loss in the phantom medium is greater than the free spaces due to increased propagation loss and scattering loss in phantom medium compared to free space medium. Fig. 4 shows the corresponding VSWR characteristics for the proposed antenna model for the band of operation. The antenna achieves 2 : 1 VSWR characteristics for the operating band which is ideal for BAN applications.

Figure 3 shows simulated and measured return losses. There is a slight shift in the frequency, but the shift lies in the same band of operation. This shift in frequency may be due to difference in propagation delay in different media (Phantom/Free space).

Figure 4 shows the VSWR characteristics of proposed antenna model measured in free space and phantom which achieve a value less than 2 in the UWB and are compared with simulated results. Fig. 5 and Fig. 6 show the simulated radiation pattern characteristics of the proposed antenna with 1.16 dB gain at 4.975 GHz and 3.5 dB gain at 6.8875 GHz taken in the direction of propagation.
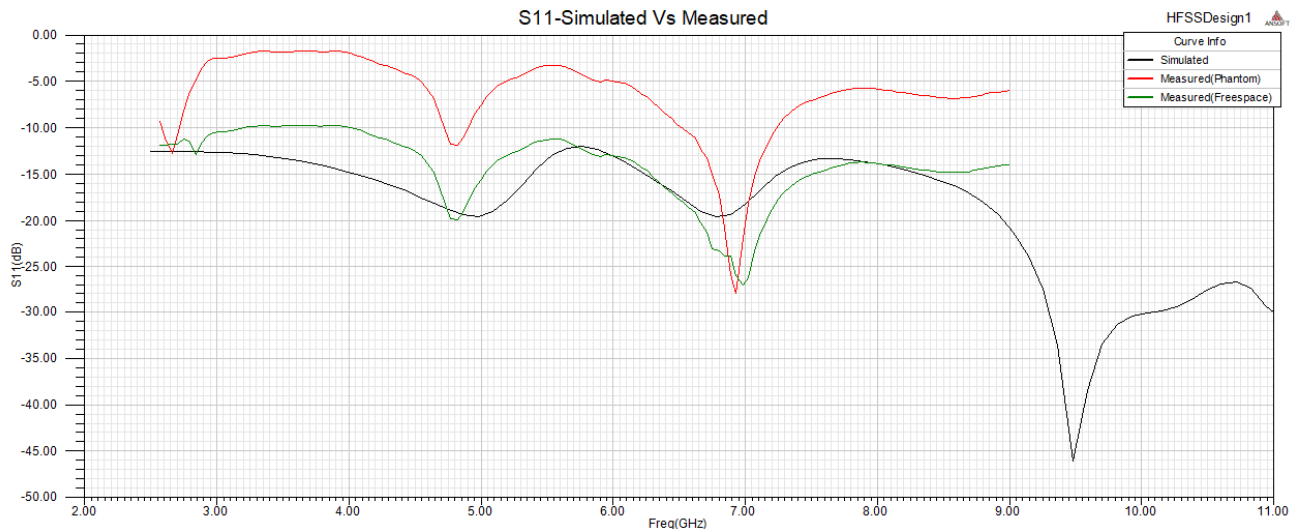

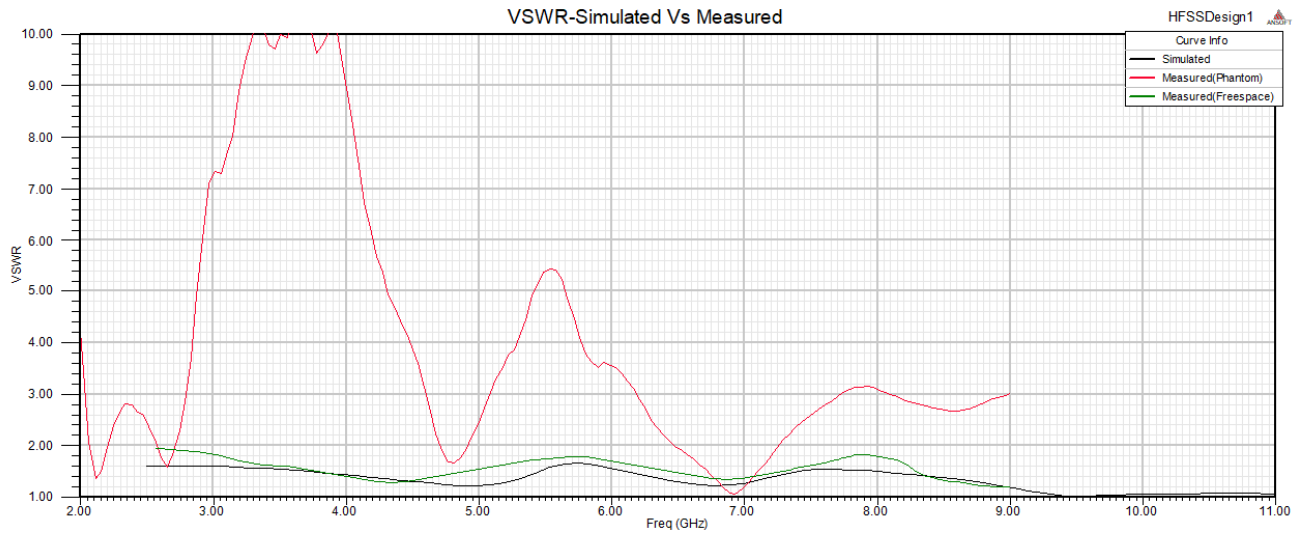**Figure 3.** Return loss (dB) — Simulated Vs measured (Phantom/Free space).

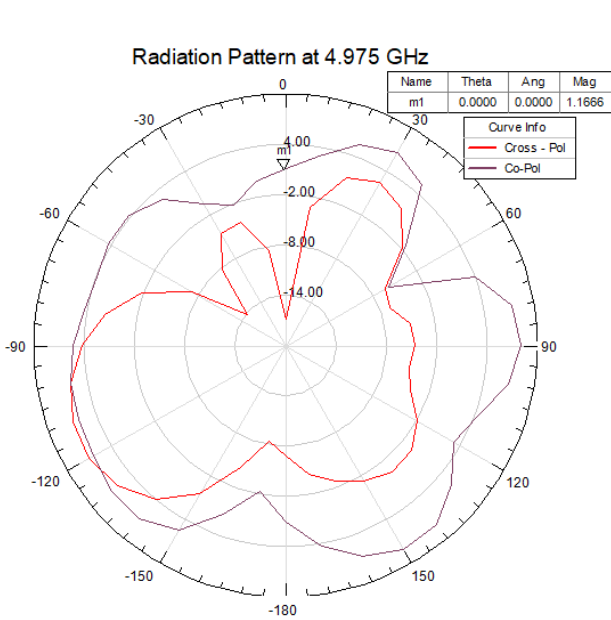**Figure 4.** VSWR — Simulated Vs measured (Phantom/Free space).

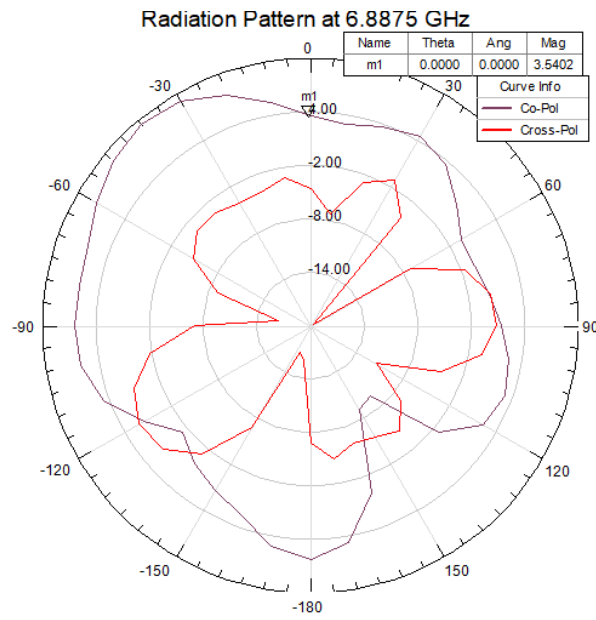**Figure 5.** Radiation pattern simulated (4.975 GHz).

Figure 6. Radiation pattern simulated (6.8875 GHz).

Table 2. Simulated Vs. Measured Results of the proposed staircase truncated antenna.

Simulation results				Measured results (In Phantom)			Measured results (Free space)		
Freq (GHz)	Return loss (dB)	VSWR	Gain	Freq (GHZ)	Return loss (dB)	VSWR	Freq (GHz)	Return Loss (dB)	VSWR
4.9750	−19.58	1.23	1.3 dB	4.8200	−11.9	1.67			
6.8875	−19.36	1.24	3.5 dB	6.9300	−28	1.07			
9.4750	−45.9	1.01	7.3 dB						
2–11	< −10	< 2					2–9	< −10	< 2

Table 2 presents the comparison of the simulated and measured results. The simulated and measured results are similar in the required band of operation.

3. SIMULATION SCENARIO

The BANsim [19], a raytracing [17, 18] based simulator that is available at the Department of Electronics and Communication Engineering of Adhiparasakthi Engineering College, Melmaruvathur, has been used for numerical simulations. The heterogeneous tissue layer between the transmitter and receiver is considered as a single multi-layer object. Numerical simulations are performed with a four-layer human abdomen model as shown in Fig. 7. The number of layers and their widths have been varied according to the location of the receiving antenna.

In the case of on-body vs. in-body communication, no direct path is available since either the transmitting antenna or receiving antenna will be an implantable one. Instead, the Line Of Sight (LOS) path is replaced with Direct Transmitted Ray (DTR) path, and the intensity of the electric filed of DTR from the transmitter to the receiver is evaluated by incorporating the ABCD matrix [16] in the
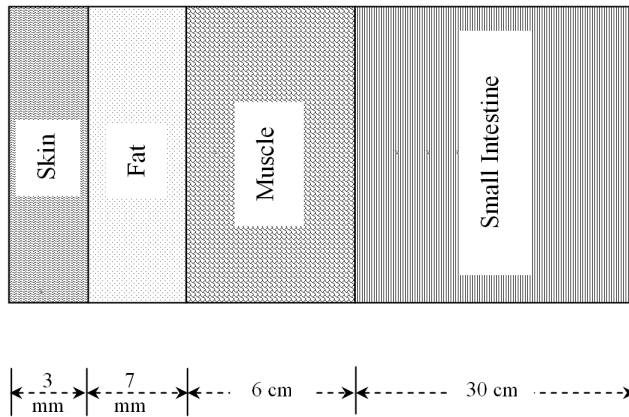
Figure 7. Cross section of the four layer model of human abdomen.
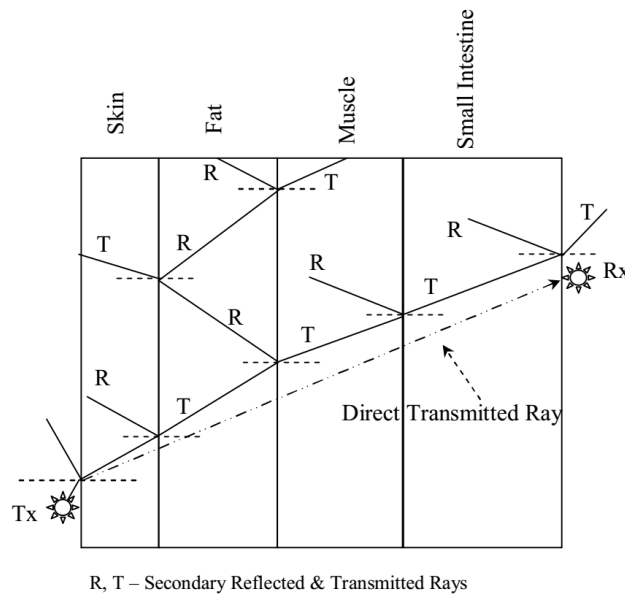
Figure 8. Ray tracing in tissue layers of human abdomen model.

scattering coefficient calculation.

Next, the rays are emitted from the transmitter, and all the points of intersection and the direction vectors of secondary reflected rays and secondary transmitted rays (STR) are found using the ray tracing technique as shown in Fig. 8. Ray tracing is proceeded with the secondary rays separately. This type of recursive ray-tracing procedure is continued further.

The transmitter is placed at the surface of the human skin, and the receiving antenna is moved through the four layers. Maximum of ten reflections and transmissions are included in the simulation. Path loss is calculated at 1 mm interval up to a depth of 30 cm in the abdomen region.

4. PATHLOSS MEASUREMENTS WITH THE LIQUID PHANTOM

Validating the applicability of the proposed antenna design for UWB is of interest, and hence path loss has been measured in a honey based liquid phantom [19], which mimics the human abdomen, with a Key sight N9917A Vector Network Analyzer (VNA) that is available at Microwave Lab of BSACIST, Chennai. Standard UWB test antenna that is supplied with VNA is used as transmitting antenna, and the proposed antenna is used as receiving antenna. Receiving antenna is insulated with a polythene
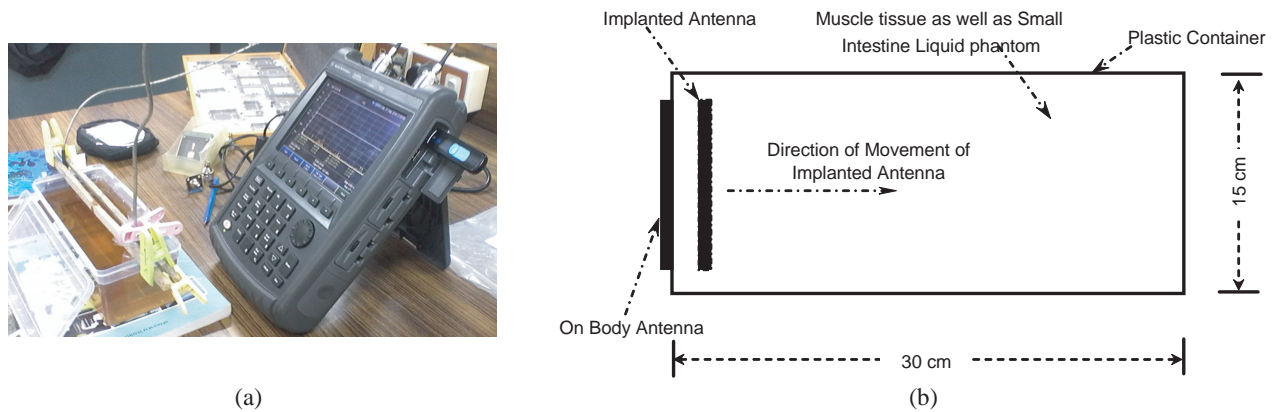

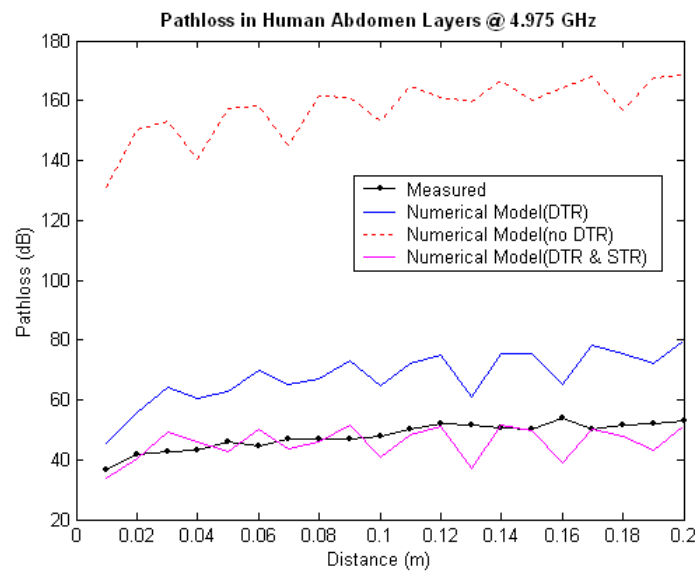**Figure 9.** (a) Measurement setup. (b) Measurement setup.

Figure 10. Path loss in the four layer human abdomen model at 4.975 GHz.

cover of 0.5 mm thickness, in order to avoid any shorts. The measurement setup is shown in Figs. 9(a) and 9(b). The path loss at different depths is measured in terms of S_{21} parameter and compared with that of simulations.

The path loss characteristics of human abdomen that is predicted using the numerical simulation at 4.975 GHz and 6.8875 GHz are plotted in Fig. 10 and Fig. 11 and compared with the measurements made in honey based liquid phantoms in the respective frequencies. Though a homogeneous liquid phantom has been used, good agreement is found between measured and predicted path loss characteristics. This is due to the low attenuation constant of skin and fat layers whereas in muscle and small intestine layers it is high [11]. As the movement of receiving antenna was done manually, deviation around the predicted results was observed in the field intensity measurements. This is because of the mismatches in the antenna orientation, which is due to the manual placement of transmitting and receiving antennas. Simulated results without direct transmitted ray is also included in the figure to study the significance of received field strength due to DTR path.
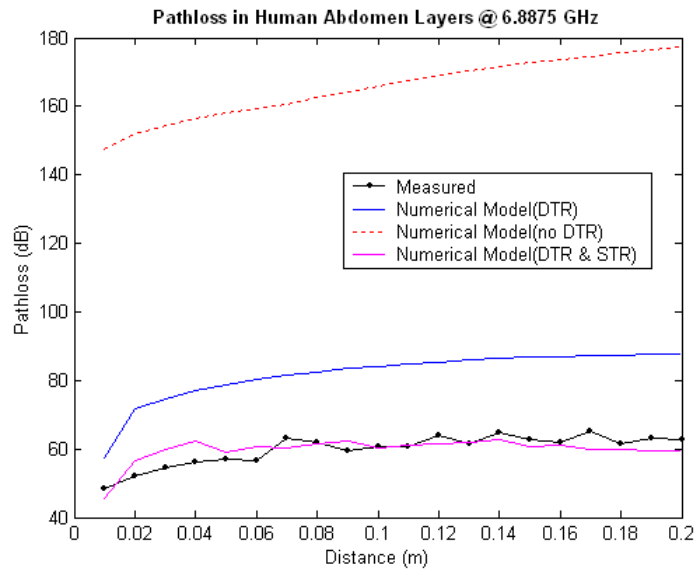

Figure 11. Path loss in the four layer human abdomen model at 6.8875 GHz.

5. SUMMARY AND CONCLUSIONS

The designed antenna works well for WLAN and satellite applications in UWB frequency range. Since UWB frequency is suitable for in-body and in-body communications this antenna, as an extension, has been used and tested for this application. The simulated path loss characteristics of human abdomen as a function of distance between the antennas at randomly selected UWB frequencies are compared with the measurements made in honey based liquid phantoms in the respective frequencies. Excellent agreement is found between measured and predicted path loss characteristics. In the skin and fat layers path loss is less whereas in muscle and small intestine layers it is high. This is due to the high attenuation constant of muscle and small intestine layers. It is observed that for larger antenna separation, the increment in the path loss is more prominent.

REFERENCES

1. Chavez-Santiago, R. and I. Balasingham, "Ultra wideband signals in medicine [life sciences]," *IEEE Signal Process. Mag.*, Vol. 31, No. 6, 130–136, Nov. 2014.

2. Zastrow, E., S. K. Davis, and S. C. Hagness, "Safety assessment of breast cancer detection via ultra-wide band microwave radar operating in pulsed radiation mode," *Microwave Optical Technology Letters*, Vol. 49, No. 1, 221–225, Jan. 2007.

3. Otto, C., A. Milenkovic, C. Sanders, and E. Jovanov, "System architecture of a wireless body area sensor network for ubiquitous health monitoring," *Journal of Mobile Multimedia*, Vol. 1, No. 4, 307–326, 2006.

4. Tang, M.-C., R. W. Ziolkowski, and S. Xiao, "Compact hyper-band printed slot antenna with stable radiation properties," *IEEE Transactions on Antennas and Propagation*, Vol. 62, No. 6, Jun. 2014.

5. Li, P., J. Liang, and X. Chen, "Study of printed elliptical/circular slot antennas for ultrawideband applications," *IEEE Transactions on Antennas and Propagation*, Vol. 54, No. 6, 1670–1675, Jun. 2006.

6. Chen, W.-L., G.-M. Wang, and C.-X. Zhang, "Bandwidth enhancement of a micro strip-line-fed printed wide-slot antenna with a fractal-shaped slot," *IEEE Transactions on Antennas and Propagation*, Vol. 57, No. 7, 2176–2179, Jul. 2009.

7. Wang, J. and Q. Wang, "Channel modeling and BER performance of an implant UWB body area link," *Proceedings of Second International Symposium on Applied Sciences in Biomedical and Communication Technology (ISABEL'09)*, Bratislava, Slovak Republic, 2009.

8. Nagaoka, T., S. Watanabe, K. Saurai, E. Kunieda, S. Watanabe, M. Taki, and Y. Yamanaka, "Development of realistic high resolution whole-body voxel models of Japanese adult males and females of average height and weight, and application of models to radio-frequency electromagnetic-field dosimetry," *Phys. Med. Biol.*, Vol. 49, 1–15, 2004.

9. Khaleghi, A., R. Chavez-Santiago, X. Liang, I. Balasingham, V. C. M. Leung, and T. A. Ramstad, "On ultra-wide band channel modeling for in-body communications," *Proceedings of Fifth IEEE International Symposium on Wireless Pervasive Computing (ISWPC)*, 140–145, Modena, Italy, May 5–10, 2010.

10. Khaleghi, A., R. Chavez-Santiago, and I. Balasingham, "Ultra-wideband statistical propagation channel model for implant sensors in the human chest," *IET Microwaves, Antennas & Propagation*, Vol. 5, No. 15, 1805–1812, 2011.

11. Gabriel, C., "Compilation of the dielectric properties of body tissues at RF and microwave frequencies," *Brooks Air Force*, N.AL/OE-TR-1996-0037, San Antonio, TX, 1996.

12. Khaleghi, A., R. Chavez-Santiago, and I. Balasingham, "An improved ultra-wide band channel model including the frequency-dependent attenuation for in-body communications," *Proc. IEEE 34th Annu. Int. Conf. Eng. Med. Biol. Soc.*, 1631–1634, San Diego, CA, USA, 2012.

13. Støa, S., R. Chavez-Santiago, and I. Balasingham, "An ultra-wide band communication channel model for the abdominal region," *Proc. IEEE Globecom 2010 Workshop on Advanced Sensor Integration Technology (ASIT 2010)*, Miami, Florida, USA, Dec. 2010.

14. Støa, S., R. Chavez-Santiago, and I. Balasingham, "An ultra wideband communication channel model for capsule endoscopy," *IEEE*, 2010.

15. Floor, P. A., R. Chávez-Santiago, S. Brovoll, Ø. Aardal, J. Bergsland, O.-J. H. N. Grymyr, P. S. Halvorsen, R. Palomar, D. Plettemeier, S.-E. Hamran, T. A. Ramstad, and I. Balasingham, "In-body to on-body ultra wideband propagation model derived from measurements in living animals," *IEEE Journal of Biomedical and Health Informatics*, Vol. 19, No. 3, 938–948, 2015.

16. Ishimaru, A., *Electromagnetic Wave Propagation, Radiation, and Scattering*, Prentice Hall, New Jersey, 1991.

17. Seidel, S. Y. and T. S. Rappaport, 'Site-specific propagation prediction for wireless in-building personal communication system design," *IEEE Transactions on Vehicular Technology*, Vol. 43, No. 4, 879–891, 1994.

18. Rappaport, T. S., *Wireless Communications Principles and Practice*, Prentice Hall, New Jersey, 2002.

19. Thirumaraiselvan, P. and S. Jayashri, 'Numerical modelling of ultra wide band signal propagation in human abdominal region," *International Journal of Biomedical Engineering and Technology (IJBET)*, Vol. 27, No. 1/2, 17–32, 2018.